Last Glacial Maximum glaciation of the central South Carpathian range (Romania)

Joachim KUHLEMANN[1)2)*)], Florentina DOBRE[2)], Petru URDEA[3)], Ingrid KRUMREI[2)],
Emil GACHEV[4)], Peter KUBIK[5)] & Meinert RAHN[1)]

[1)] Swiss Nuclear Safety Inspectorate ENSI, Industriestrasse 19, 5200 Brugg, Switzerland;

[2)] Institute for Geosciences, University of Tübingen, Tübingen, Germany;

[3)] Department of Geography, West University of Timisoara, Romania;

[4)] Department of Geography, Ecology & Environment protection, SW University Blagoevgrad, Bulgaria;

[5)] Laboratory of Ion Beam Physics, ETH Zürich, Zürich, Switzerland;

[*)] Corresponding author, kuj@ensi.ch

Abstract

Glacial moraines in the central South Carpathian Range (Făgăraş Mountains, Romania) have been mapped in order to reconstruct the elevation of the climatic snowline (ELA) during the Last Glacial Maximum (LGM). In a representative north-south cross-section, depositional ages of moraine complexes have been determined by 10Be exposure dating. In the study area, the ELA of the LGM is similar both in southerly and in northerly exposition. By contrast, in the Younger Dryas Stade the ELA was about 150 m lower in northerly as compared to southerly exposition, typical for an almost symmetric precipitation as at present, the higher southerly ELA reflecting the effect of aspect of preferential moisture supply. The ELA distribution of the LGM along the range shows a depression in the wet southwest and a rise in the dry northeast. This pattern suggests a preferential winterly moisture advection from the southwest, which gradually changed to a westerly advection of moisture causing a roughly symmetric precipitation during the late glacial, approaching present conditions.

Im zentralen Abschnitt der Südkarpaten (Făgăraş-Massiv, Rumänien) wurden glazigene Moränen kartiert, um die Höhe der klimatischen Schneegrenze (ELA) im Letzten Glazialen Maximum (LGM) zu rekonstruieren. In einem repräsentativen Nord-Süd-Querprofil wurden Ablagerungsalter mit 10Be-Expositionsaltern bestimmt. In diesem zentralen Abschnitt der Südkarpaten befand sich die ELA im LGM sowohl in südlicher als auch in nördlicher Exposition in gleicher Höhe. Im Gegensatz dazu war die ELA in der Kaltphase der Jüngeren Dryas in nördlicher Exposition 150 m tiefer als in südlicher Exposition. Das ist typisch für eine etwa symmetrische Niederschlagsverteilung ähnlich wie heute und spiegelt den Effekt der Exposition wider. Die ELA-Verteilung entlang der Gebirgsachse im LGM zeigt eine Depression im feuchten Südwesten und einen Anstieg im trockenen Nordosten. Diese Verteilung deutet auf eine damalige Feuchteanlieferung aus Südwesten, die sich im Verlauf des Spätglazials auf eine westliche Richtung veränderte und die im LGM asymmetrische in eine näherungsweise symmetrische Feuchteverteilung umwandelte, die sich modernen Verhältnissen annäherte.

1. Introduction

Mountain climate reconstructions in the geological past provide evidence of atmospheric processes at mid-tropospheric elevations and contribute a vertical dimension to various data sets generated from marine and terrestrial archives from near-coast sites (e.g., Kuhlemann et al., 2008). An increasing spatial coverage of palaeoclimate evidence of circum-Mediterranean mountains is available for maximum glacier expansions during cold spells (Hughes et al., 2006; Hughes and Woodward, 2008; Hughes et al., 2013). Semi-continental scale proxy-data coverage is essential to validate coupled ocean-atmosphere circulation models of higher resolution (e.g. Jost et al., 2005).

For a better understanding of regional climatic response to rapid climate change during cold spells, particularly moisture transport, the Last Glacial Maximum (LGM, 24-18 ka) represents the best studied time slice. Numerous studies on fast changes of marine climate are available for the North Atlantic Ocean, and recent studies in the western Mediterranean have demonstrated a causal link and immediate response of sea

surface temperatures (SST) and Greenland temperatures (Cacho et al., 2001, 2002; Meland et al., 2005). It has been shown that cold spells in the Mediterranean have been related to melt water breakouts in the North Atlantic Ocean (Heinrich events). The Heinrich events discussed in this paper are HE2, preceding the LGM, HE1 (Oldest and Older Dryas Stade) and HE0 (Younger Dryas Stade; Cacho et al., 2001, 2002). Dramatic short-term cooling especially affected the western Mediterranean basin, whereas the central and eastern Mediterranean basins were less affected (Hayes et al., 2005; Kuhlemann et al., 2008). This raises the question, if preferential north-directed flow of relatively warm air over the Aegean Sea was pushed by south-directed flow of cold air in the western Mediterranean basin, as part of a meridional lobate atmospheric circulation system. In this case, the target area, located within south-eastern Europe (Fig. 1), should have been characterised by a relatively high climatic snowline (= equilibrium line altitude, ELA) in the Mediterranean LGM context, caused by preferential southerly advection (Kuhlemann et al.,

2008). Such a scenario is already indicated in the ELA map of Messerli (1967). The latter map is entirely based on undated moraine relics.

In the continental scale of LGM climate, possible blocking of westerly moisture supply by central European high pressure raises the question to which degree the Fennoscandian ice shield was supplied from the south. Florineth and Schlüchter (1998, 2000) assume moisture supply along a cyclone track from the southwestern Mediterranean basin across central Italy and the Pannonian basin to the N (Fig. 2). Lake levels during the LGM indicate relatively wet conditions in southern Spain, Greece, and southern Turkey; whereas central Italy remained relatively dry (Harrison et al., 1996). The eastern part of the Eastern Alps and the western Pannonian Basin also remained relatively dry (Van Husen, 1997), which has recently been confirmed by Kerschner and Ivy-Ochs (2007) and explained by the regional width of the orogen. According to modern polar cyclone tracks in the Mediterranean, an eastward continuation of Mediterranean cyclones across the southern Dinarides or Greece to the western Black Sea and a subsequent turn to the NNW and N may be more typical for a moisture supply of the southern Fennoscandian ice shield.

For testing the hypothesis of more frequent meridional winter circulation during the LGM in the Mediterranean, a stratigraphic framework for the mountains of south-eastern Europe is essential, in order to trace cyclone tracks and moisture transport in the LGM. The highest massif in Romania in the central part of the South Carpathians (Făgăraş Mountains) provides proper conditions for a detection of north-south and west-east gradients of precipitation during cold spells. The primary aim of this paper is to track the regional W-E gradient of moisture supply by mapping of the ELA in the LGM. The second aim is to study the N-S ELA gradient in a representative cross section from the LGM to the Younger Dryas Stade, in order to constrain temporal changes.

2. Regional setting

The Carpathian mountain range forms an external fold and thrust belt largely composed of sedimentary rocks and an internal belt of mainly low-grade metamorphic metasediments (Kräutner, 1991, 1997). The Southern Carpathians, or Transylvanian Alps, are the highest mountain chain of the Romanian Carpathians, with 11 peaks higher than 2500 m a.s.l., the hig-
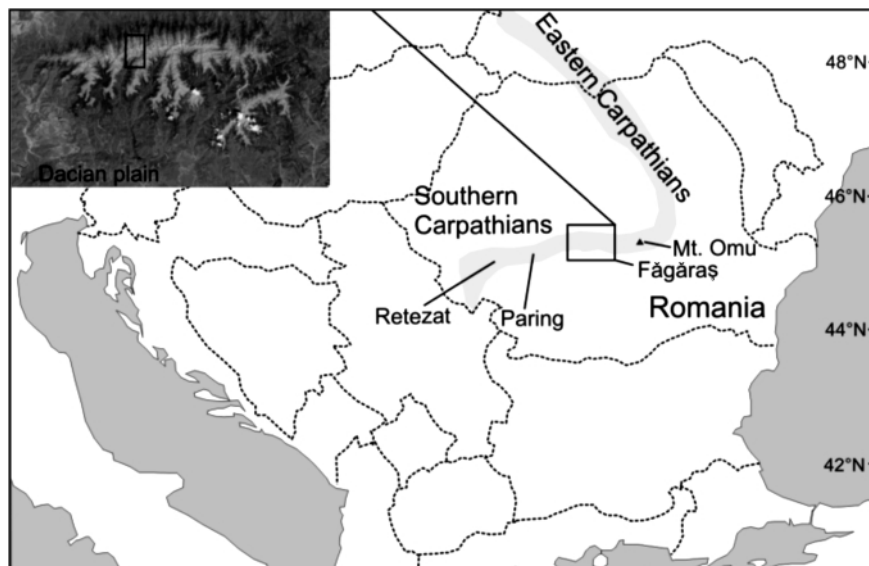

FIGURE 1: Sketch map of southeastern Europe with the location of the study area (black box in upper left inset).
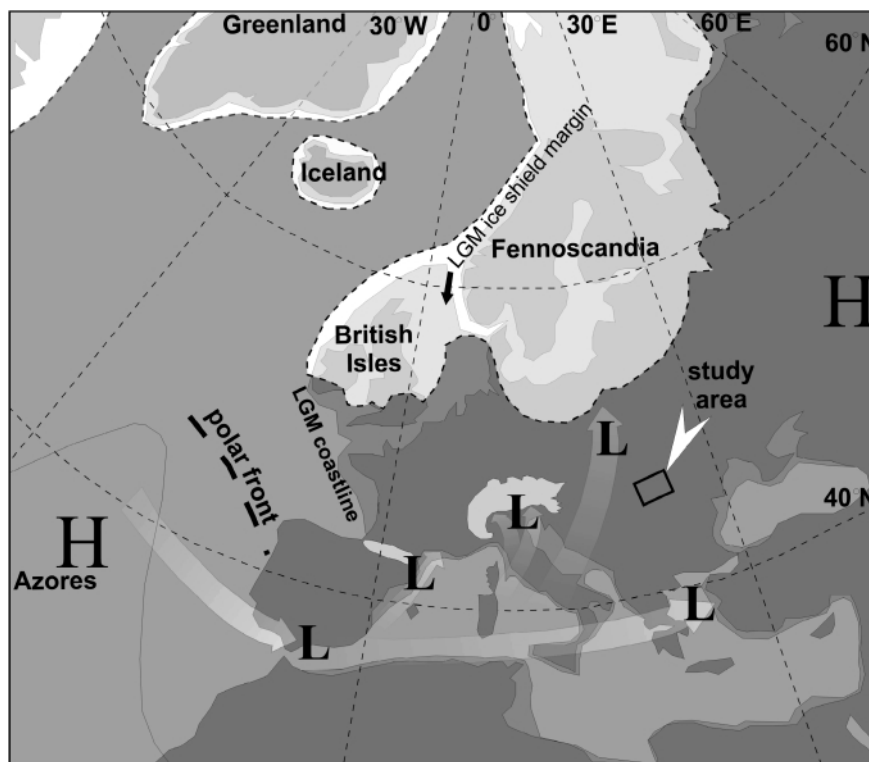

FIGURE 2: Preferential Mediterranean cyclone tracks (L) and anticyclone (H) distribution during the Last Glacial Maximum according to Florineth and Schlüchter (2000). The outline of the Fennoscandian ice shield is adopted from Svendsen et al. (2004). Dark outlines: present-day land distribution, medium grey coastal zones show LGM coastline.

hest peak, Moldoveanu (2544 m), located in the Făgăraş Mountains. Exposed rocks in the Făgăraş include quartz-rich polyphase low- to medium-grade metamorphic rocks, especially gneisses. The Făgăraş massif in general forms an asymmetric west-east trending anticline with a crystalline core. It experienced rapid late Miocene uplift and exhumation (Zweigel et al., 1998, Sanders et al., 1999). Thermochronological data from altitudes above 2000 m indicate that the summit planation surface (Fig. 3) has cooled to surface conditions already in Miocene times (Moser et al., 2005).

In the Făgăraş massif, peaks higher than 2500 m rise above a south-exposed 50 km-wide toe of forested uplands, which southward decline into the Romanian Plain, a part of the Dacian Basin. The higher mountain range exhibits glacial sculpture, with cirques, steep slopes and glacially shaped valleys, associated either with sharp peaks and ridges. Despite for glacially formed jagged Alpine relief in the axial part, small remnants of palaeorelief survived at the level of the summits and on long ridges trending southward, still reflecting the shape of the underlying structural anticline. The main drainage divide is located only in 10 to 12 km distance south of the Transylvanian basin, situated at 500 m average altitude. The contrast between narrow-spaced north-exposed steep valleys and relatively wide south-exposed valleys (middle and lower parts) with several tributary cirques seems to be related to either steep (north) or shallow (south) dip of schistosity and bedding of meta-sediments. Detailed geomorphic observations with special recognition of glacial features and rock glaciers are provided by Posea (1981), Urdea (1992, 2000, 2004), Florea (1998) and Nedelea (2004, all in Romanian language), and Horedt (1988b). The former existence of Pleistocene glaciers in the Făgăraş Mountains was first noted over 125 years ago by Lehmann (1881, 1885). Recently, the aspect and altitude of glacial cirques in the mountains of Romania has been used to postulate a preferential winterly moisture supply from the northwest (Mîndrescu et al., 2010).

Recent climate conditions are moderately continental with an annual average of -2.5 ºC temperature at 2500 m altitude, which is similar to the Eastern Alps. Precipitation shows a moderate gradient from the dryer east (Omu Peak 2505 m: 1277 mm/a) to the relatively moist west (Parâng massif, 1585 m: 1400 mm/a, Urdea, 2000). Moisture is typically advected from SW to NW directions, and the amount of precipitation is almost similar (symmetric) on both flanks of the range. The post-glacial climate history of SW Romania has been assessed by the PP10 stalagmite from Poleva Cave (Locvei Mountains), which confirms a gradual warming in the Holocene with several warm events such as those around 5.2 and 3.3 ka, punctuated by cool episodes by c. 8, 7.2 and 4.2 ka (Constantin et al., 2006).

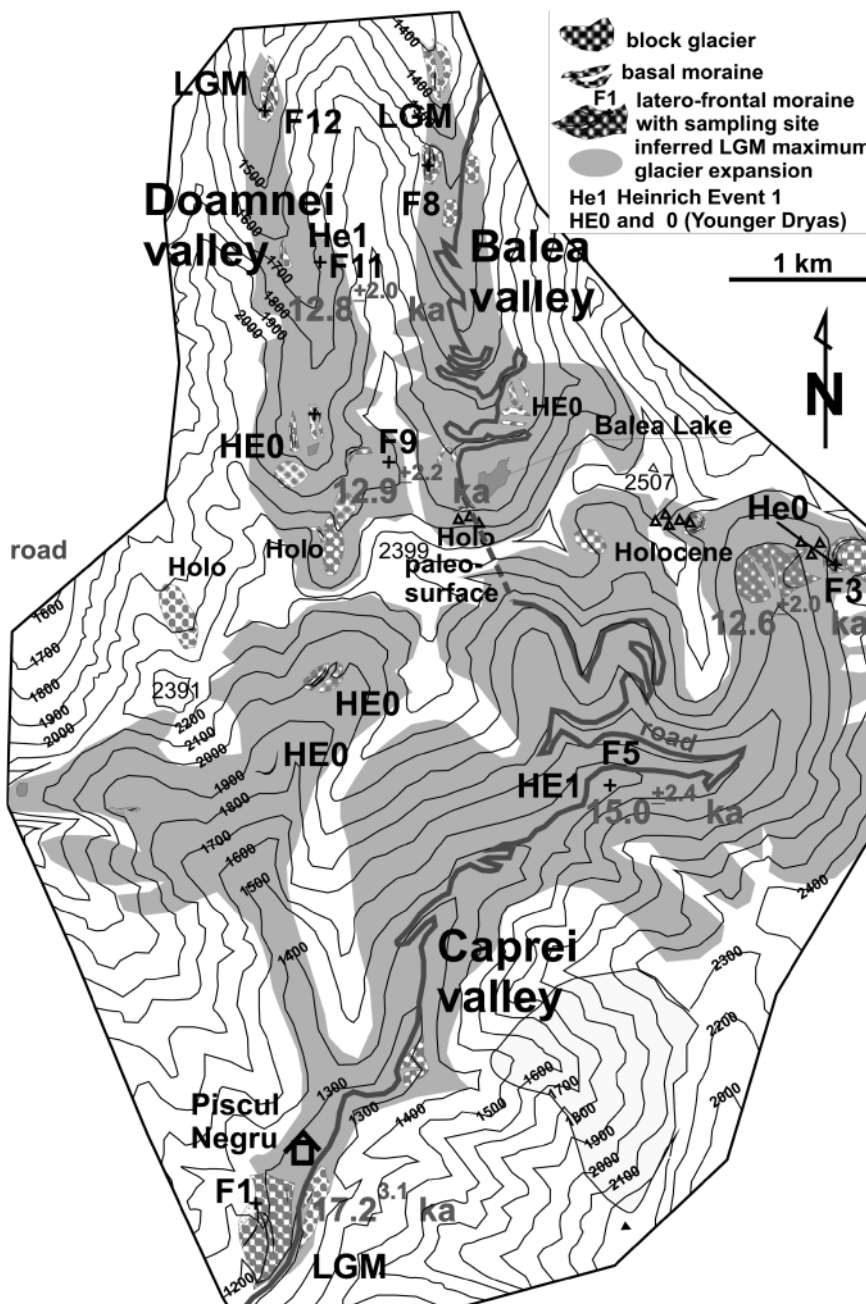Recently published exposure ages from the Retezat massif at the wes-

Figure 3: Local sketch map of the central Făgăraş section with sampling locations and glacier deposits (location in Fig. 1). Holo means Holocene.

field code	altitude [m a.s.l.]	lat [° N]	long [° E]	Qz [g]	[10]Be [a] at/g [1E+4]	analyt. error [%]	local production rate[b] [at/g/a]	topogr. shielding	age [kyr] corr. [c]	error [ka][d]	age [ka] no erosion[e]
F1	1306	45.55	24.60	32.02	16.79	8.3	12.27	0.979	17.4	3.2	14.2
F3	2063	45.60	24.65	31.67	23.26	6.5	21.60	0.970	12.8	2.0	11.0
F5	1610	45.58	24.63	33.08	18.65	5.9	15.19	0.955	15.1	2.4	12.7
F9	2065	45.60	24.61	30.93	23.41	8.5	21.30	0.955	13.1	2.3	11.2
F11	1670	45.62	24.60	32.76	13.83	6.0	12.80	0.769	13.0	2.0	11.1

[a] Blank corrected.
[b] Local production rate for spallation.
[c] Correction includes sample thickness, topographic shielding, geomagnetic variations, atmospheric pressure and erosion.
[d] 1σ-uncertainty including analytical and systematic errors.
[e] Age calculation includes only correction for sample thickness, topography, geomagnetic variations and atmospheric pressure.

Table 1: Sample information, results of [10]Be measurements and calculated exposure ages, based on the calculation sheet of Balco et al. (2008). Exposure ages are calculated by assuming 5 mm/ka of erosion and an average sample thickness of 3 cm and an air pressure of 1020 hPa.

tern termination of the South Carpathians show an ELA of about 1800 m (accumulation area ratio (AAR) = 0.67) for the Lolaia glacier advance (undated, Rissian or Early Wuermian) and about 1850 m for the Last Glacial Maximum (LGM), which has been dated at an untypically young age centred at 16 ka (Reuther et al., 2004, 2007). These authors assume an increase of available moisture in the late glacial to explain this local retardation to the superimposed European and northern hemispheric trend. As compared to the estimated modern snowline of 2900 m (Horedt, 1988a), Reuther et al. (2004) calculate an ELA depression of 1050 m in the LGM. Messerli (1967) estimates an ELA of 1900 m for the entire range in the LGM.

3. Methods

3.1 Exposure age dating

Exposure dating has been performed by analysing in situ-produced cosmogenic 10Be in quartz of metamorphic rocks. Exposure dating is based on the assumption that rock surfaces like that of a glacial boulder are totally reset (at least 2 m of rock abraded for almost total reset) and exposed to cosmic rays ever since melting of glaciers. Hence, the samples were taken from the topmost 1-2 centimetres of bedrock surfaces or of glacial boulders, which rose at least 1.5 m above the surrounding regolith to exclude temporal soil cover of the exposed rock. Chemical treatment of samples generally followed Kohl and Nishiizumi (1992). Purified quartz samples of 31 to 33 grams were prepared for Accelerator Mass Spectrometry (AMS) measurements at Tübingen after von Blanckenburg et al. (2004), and measured at ETH Zürich. Originally, the measured 10Be/9Be ratios were normalized to the standard S555 with a nominal value of 95.5[-12] using a [10]Be half-life of 1.51 Myr. Recently the use of a [10]Be half-life of 1.387 Myr is recommended (Korschinek et al. 2009; Chmeleff et al. 2010). The in-house AMS Be standards at Zürich were re-calculated and converted to the new system (Kubik and Christl, 2010) to allow for better comparisons with AMS results from other laboratories. We also converted the AMS measurement data to the new half-life (Kubik and Christl, 2010).

For the calculation of exposure ages and erosion rates we used the CRONUS-Earth online calculator (http://hess.ess.

washington.edu/), version 2.2 (Balco et al., 2008). The new half-life is incorporated into this version and the normalization of the measurements is taken into account. The calculator uses the value of 160 g/cm^{2} for the attenuation length of production by spallation in rock and an exponential depth dependence. Local surface production rates are scaled after Stone (2000). From the five offered scaling schemes for spallogenic production we chose the one after Dunai (2001) in order to keep them comparable in a Mediterranean framework (Kuhlemann et al. 2008). Hence, the production rate for spallation is 4.90 ± 0.56 at/g yr (Balco et al. 2008). The exposure ages (Tab. 1) are corrected for variations in the geomagnetic field, topographic shielding, erosion and air pressure.

The shielding values were measured in the field. Elevation and latitude were determined from 1:50'000 topographic maps. We assume that 15 mm/ka for feldspar-bearing quartz schists and gneisses is a reasonable estimate for the erosion rate in the study area considering the following aspects:

Weathering rates are quite variable and range between 2 and 20 mm/ka for granite of different degree of micro-fracturing, late stage epizonal cementation (chlorite, quartz), anorthite/biotite-content, and climate (Kuhlemann et al., 2007). We here refer to rates used by Small et al. (1997), particularly based on the minimum weathering rates obtained by these authors for the Sierra Nevada (USA).

Air pressure should be included in exposure age calculation on the base of climate models of the past although such results can hardly be validated with proxy-data. Summer air pressure is in the range of 1013 hPa at present.

Snow cover in the past is virtually impossible to calculate in the study region. Above 20 to 30 cm of annual average effective water column, shielding is significantly younging exposure ages by 10 % and more (Schildgen et al., 2005). The problem increases with increasing elevation. Sites of late glacial deposits are potentially more affected than those of the LGM in the forested parts of the valleys, where the effect is negligible. An extensive discussion of dating uncertainties is provided, e.g., by Ivy-Ochs et al. (2007).

3.2 Palaeoprecipitation

Our assessment of palaeoprecipitation roughly follows the

approach of Kerschner et al. (2000) for the Eastern Alps. Relative differences of palaeoprecipitation at higher elevations during cold glacial stages have been calculated by reconstruction of the equilibrium line altitude (ELA) on the base of the glacier margins, as constrained by trimlines and moraines. The size of the ablation area (1/3 to 1/2) relative to accumulation area (1/2 to 2/3) of a glacier (accumulation area ratio-method; AAR) is a good approximation of the ELA (Porter, 2001), but it depends on the hypsometry of the basin and the glacier surface, and debris cover of the tongue. For a typical hypsometry of Wuermian glaciers, we chose an AAR of 0.67, according to moderately continental climate in the Carpathians (see Reuther et al., 2004, 2007). This value is recently confirmed for Alpine glaciers by mass balance calculations of the last 30 years (Zemp et al., 2007).

4. Field evidence and exposure ages

During numerous field seasons a map of low-elevation well-preserved moraines has been established in a regional stratigraphic framework by P. Urdea by valley-to-valley correlation. The ELA of the mapped outline of glaciers has been calcula-

Figure 4: Boulder F1 in the Capra valley, resting on the flat top of a terminal moraine complex which downward spreads into 4 ridges. Note that the boulder is strongly weathered but in a stable position which makes a post-depositional rotation unlikely.

ted using an Arc-GIS platform (ArcView9.2) with an underlying SRTM digital elevation model (DEM).

Within the selected N-S transect (see Fig. 5), 3 valleys have been studied in detail (Fig. 3). Two of them, the Capra and Doamnei valleys, are characterised by voluminous latero-terminal low-elevation moraines of fair morphological state of preservation with up to 4 separated individual ridges (Fig. 4). Since valleys exposed to the north are narrow and steep, the outline of ancient glaciers in map view strongly differs from the complex pattern of tributary glaciers on the southern flank of the Făgăraş. Here, similar sets of moraines are found in the forest at some 100 m lower elevation (~1700 m) as compared to the north-exposed valleys. Nevertheless, the larger catchment area of the south-exposed former glacier, particularly in the level of the cirques, results in an ELA of about 1800 m after AAR calculation.

Urdea (2004) has correlated late Wuermian glacier advances of HE1 and HE0 in the South Carpathians with the Alps and the High Tatra Mountains (Western Carpathians). Numerous of these advances have received different local names and they have been provisionally grouped according to altitudes in the entire South Carpathians.

Fieldwork in the selected N-S section has provided samples from moraine sets found at elevations described within the provisional stratigraphic system. This includes the mentioned group of large moraines between 1200 and 1500 m, a group of small moraines at 1600 to 1700 m, and a group between 1850 and 2050 m. Very small moraines or rather accumulations of angular boulders – in many cases typical rock glaciers - are found in hidden cirques above 2100 m and at the foot of steep slopes, surrounding small depressions. These features partly represent nivation hollows rather than moraine relics of niche glaciers. Boulders of sufficient size (>1.5 m above soil, stable position) are very rare and partly absent. In such cases, roches moutonnées above and partly surrounded by latero-terminal moraines have been sampled.

Three samples from the lowest and thus oldest moraine complex were measurable. Sample F12 from the north-exposed Doamnei valley yielded an age of 4.1 ± 0.6 ka, indicating late transport, probably block rotation. Glacial boulders in this moraine complex in the forest were partly outwashed and some
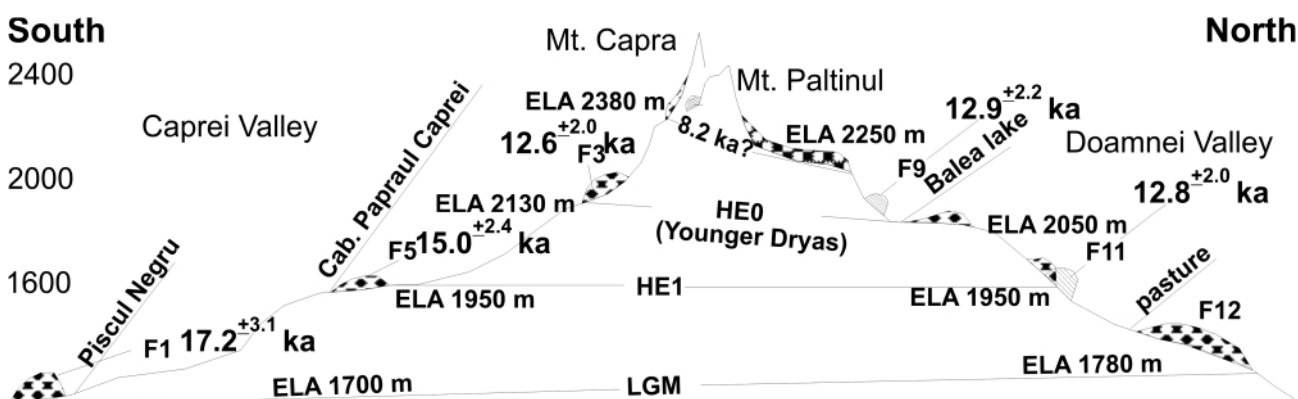
Figure 5: Schematic N-S cross section of the central Făgăraş with sampling sites and exposure ages.

trees grow on boulders. Block rotation may have been caused by falling of such a tree (Ivy-Ochs et al., 2007). Therefore, this sample is not listed in Table 1. F11 from a steep roche moutonnée in the Doamnei valley yielded 12.8±1.5 ka. The valley geometry suggests that the glacier which shaped site F11 ended at site F12. We cannot rule out that the sampled site has been shielded by some moraine cover.

Sample F1 from the Capra valley (Fig. 4) yielded 17.4±3.2 ka. This large boulder on the outwashed plain top of a large and complex moraine ridge has hardly been tilted and former coverage by moraine material should have disappeared during final melting of the glacier. The exposure age matches the LGM depositional age within error between 24 and 18 ka (Bard et al., 2000). Despite of its fair preservation and impressive volume, Urdea (2004) assumes an early Wuermian depositional age (~ 60 ka) of this latero-terminal moraine complex. The proposed Rissian Capra glacier descended to 1130 m a.s.l., at which altitude the character of a glacial trough disappears. However, thermochronological data indicate late Miocene uplift in the range of 2 km (Zweigel et al., 1998; Moser et al., 2005, see also Mîndrescu et al., 2010), implying average long-term valley incision rates of at least 0.2 mm/a, probably higher in the Quaternary (Mîndrescu et al., 2010). Since this incision rate is equivalent to at least 28 m of post-Rissian solid rock incision, a Rissian depositional age of the sampled moraine set seems highly unlikely. The creek at this site incised about 5 m of basal moraine and 1 to 2 m of solid rock, which indicates minor post-Wuermian incision and a LGM age of moraine deposition.

One sample from the middle moraine complex has been measured. F5 from the Capra valley yielded 15.1±2.4 ka. The sampled boulder was about 1.2 m high above the soil, just at the required minimum size for late glacial deposits. The age matches HE1 time of deposition within error, between 16.7

and 14.8 ka (Bond et al., 1997).

Two samples were measured from the upper moraine complex. F3 was taken from a large boulder on a steep horizontal moraine ridge surrounding a glacial depression now almost filled with a younger rock glacier. Close to and below this ridge, another latero-terminal ridge has formed somewhat earlier on a slope when the glacier had overridden the edge of the cirque. Ist flatness indicates periglacial creep of the substrate, and no larger boulder is exposed. The large moraine boulder seems to be in a stable position since deposition, and a former cover by moraine material is highly unlikely. This boulder yielded an exposure age of 12.8±2.0 ka. Sample F9 of a roche moutonnée in the upper Doamnei valley yields 13.1±2.3 ka. These ages match the glaciation of HE0, within 12.800 and 11.700 ka (Severinghaus & Brook, 1999).

If the erosion correction for the exposure ages was accepted, the mentioned glacier advances between 1200 and 1500 m altitude fit to the LGM, those at altitudes between 1600 and 1700 m fit HE1, and those between 1850 and 2050 m fit to HE0. Small local moraines at higher elevation, close to the crest, are tentatively attributed to the early Holocene cold spell at 8.2 ka, which was triggered by the last meltwater breakout of the Laurentian ice shield (Bond et al., 1997).

5. Local climate implications

As displayed in Fig. 3, the postulated elevation of LGM, HE1, HE0 and early Holocene moraines indicate a change from larger glacier protrusion to lower elevations on the southern flank in the LGM to larger protrusion on the northern flank in HE1 and the early Holocene. In the LGM, the ELA is ~1700 m in southerly and ~1800 m in northerly exposure. During HE1, the ELA is found at 1950 m on both mountain flanks. During HE0, the ELA is at ~2130 m in southerly and ~2050 m in northerly exposure. In the early Holocene, small moraines are

Figure 6: Selected ELA calculations of LGM glaciers in the Făgăraş massif (black numbers), and precipitation anomalies as calculated in Tab. 2 on the base of Zemp et al. (2007). Relatively dry regions are marked in transparent yellow, whereas relatively wet regions are marked in light green. Forest in the background topographic map is dark green.

found in semi-protected setting at 2200 m in south-easterly exposition, indicating an ELA at least as high as 2400 m in southerly exposition. To the north, small lateral moraine relics between 2200 and 2100 m aside of block glaciers are interpreted as probably representing an early Holocene glacier advance with an ELA around 2250 m. The early Holocene setting would match the typical effect of stronger insolation in southerly exposition. This change from the LGM to the early Holocene would reflect a change from a preferential advection of moisture from the south (southwest) in the LGM towards an almost symmetric supply from the west, like at present. The potential existence of early Holocene moraines in the Făgăraş, however, is rather an exception since most cirques are filled with impressive rock glaciers which were probably still active in the Little Ice Age (Urdea, 1992, 2000). Especially in the case of higher and narrow cirques surrounded by steep walls, like in the uppermost cirques in the studied cross section (Fig. 5), cirque morphologies and spatial connection clearly indicate morphogenetic and morphochronologic relations between the moraines and rock glaciers. These geomorphic features constrain the evolution of the latest glaciers in the following succession: ablation complexes → debris covered glaciers, or black glaciers → ice-cored rock glaciers → debris rock glaciers or secondary rock glaciers (Urdea, 1997, 2004). In an increasingly continental climate this morphogenetic succession is typical. Apparently postglacial small cirques in the Făgăraş may appear problematic, but small glaciers were common in parts of the Balkan Mountains during the Holocene, as demonstrated for the Little Ice Age (Hughes, 2010).

Mapping of the ELA minimum in the LGM along the mountain chain shows a general rise from west to east by almost 200m both on the northern and the southern slopes (Fig. 6). This indicates drying from west to east, like at present. In the centre of the range, two high ridges trending far to the south appear to protect a narrow valley of relatively high headwaters and cirques (Vâlsan). The ELA of the Vâlsan valley was 160 m higher than that of the Izvoru Mircii valley next to the west, which appears to have captured much more moisture. In the light of the local topography this can be explained by preferential south-westerly moisture advection and enhanced precipitation in the wide and deep Izvoru Mircii valley. Similarly, moisture advected from the south is funnelled by the wide deep valleys west and east of the high topographic outlier which host the Vâlsan valley. Northeast of the high topographic outlier and north of the main drainage divide, the small Sâmbăta valley with its ELA 70 m higher than the neighbouring Valea Mare appears to be situated in the dry rain shadow of the high topographic outlier south of the main drainage divide. To the west, isolines of relative precipitation differences are tight which also favours south to southwest advection of moisture and potentially a foehn wind effect north of the main drainage divide. East-directed advection of moisture on the northern flank of the Făgăraş massif appears to have been hampered where the northward extending ridges rise above 2000 m.

In order to quantify differences in moisture supply, raw ELA data must be corrected for regional temperature differences and the influence of differences in insolation. There are no mid- or high-elevation annual average temperatures (AAT) available from the northern flank of Făgăraş, and on the southern flank

valley	ELA raw	aspect (-)	aspect-ELA correction[1] (m)	regional T_{ann}-ELA correction[2]	ELA corr. (m)	delta mean ELA 1768	pp anomaly[3] LGM (%)
Avrigelul	1670	NNW	-40	0.0-	1710	58	16
Scarii nord	1690	N	-50	0.0-	1740	28	8
Sebota Scarii	1800	N	-50	0.0-	1850	-82	-16
Negoliu	1790	NNW	-40	0.0-	1830	-62	-12
Laila	1735	N	-50	0.0-	1785	-17	-3
Bâlea	1780	N	-50	0.0-	1830	-62	-12
Albota	1710	N	-50	0.0-	1760	8	2
Ucisoara	1700	N	-50	0.0-	1750	18	5
Valea Mare	1780	N	-50	0.0-	1830	-62	-12
Sâmbata	1850	N	-50	0.0-	1900	-132	-26
Dejani	1800	N	-50	0.0-	1850	-82	-16
Topolog	1710	S	40	1.0- = +137 m	1631	137	37
Capra	1780	SSW	50	1.0- = +137 m	1693	75	20
Izvoru Mircii	1740	SSW	50	1.0- = +137 m	1653	115	31
Vâlsan	1900	S	40	1.1- = +150 m	1790	-22	-4
Leaota	1825	SE	20	1.0- = +137 m	1690	78	21
Vladu	1880	SE	20	1.0- = +137 m	1763	5	1

[1] assuming an aspect-related total range of 100 m of ELA variation due to insolation, the ELA in the S to SW quadrant is put 50 m higher than average and the N to NE quadrant is put 50 m lower
[2] annual average temperature increases to the south which rises the ELA by 137 m/1°C
[3] the precipitation anomaly is calculated from the difference of the local ELA to the expected ELA (av. ELA, 2210 m) minus aspect and Tann effect 100 m ELA depression accounts for 27 % more precipitation, 100 m ELA rise for 20% less precipitation

TABLE 2: Calculation of ELA differences and precipitation anomaly, after Zemp et al. (2007), by correction for the effects of aspect and temperature.

only the station Cozia (1577m) with an AAT of 3.0 °C is available. If stations at low elevation north of the Făgăraş massif are used for extrapolation, such as station Făgăraş at 429m with an AAT of 7.9 °C, the respective AAT would be 0.5 or 1°C at 1577 m, depending on the lapse rate (0.65 or 0.6 °C/100m, respectively). Part of the difference of 2-2.5 °C between north and south, however, is due to winterly temperature inversion in the Transylvanian basin. Hence, a minimum difference of 1 °C is tentatively assumed in analogy to the main west-east drainage divide of the "Shara Range" separating Kosovo and Macedonia (Kuhlemann et al., 2009b).

The effect of aspect (insolation) is estimated from Alpine examples in settings with roughly homogenous precipitation and has to be considered as an estimate. Assuming an aspect-related total range of 100 m of ELA variation solely caused by insolation, but not insolation-dependent temperature, the ELA in the S to SW quadrant is put 50 m higher than average and the N to NE quadrant is put 50 m lower. The pattern does not change much if other numbers are used for correction.

The precipitation anomaly is calculated from the difference of the local ELA to the expected ELA (average ELA 1736 m in the Făgăraş massif) minus aspect and AAT effect (Tab. 2). A 100 m ELA depression accounts for 27 % more precipitation, whereas a 100 m ELA rise for 20 % less precipitation (Zemp et al., 2007). Since Ohmura et al. (1992) obtained an ELA rise of 100 m by only 9 % precipitation increase, based on a global data set, the uncertainty of the present approach is high with respect to the absolute values obtained, but not for the distribution pattern of anomalies.

The resulting pattern shows what the distribution of raw ELA data already suggested: a preferential moisture advection from the south to southwest direction and the effect of the high topographic outlier south of the main drainage divide and its rain shadow effect to the northeast. Such preferential moisture advection in the LGM differs from the modern one which is preferentially from the west and results in a more or less symmetric distribution of precipitation on both flanks of the Făgăraş massif. On the other hand, a purely southerly flow in the LGM, as suspected from the Mediterranean scale atmospheric circulation, would not consider the westerly component shown above. Hence, an improved model is required for larger scale atmospheric circulation.

6. Mediterranean mountain climate during the LGM and the late glacial

A Mediterranean-wide compilation of the ELA of LGM glacier expansion has been given by Kuhlemann et al. (2008). The new map is still locally based on work compiled by Messerli (1967), particularly in southeastern Europe. Currently available ELA reconstructions for the Wuermian maximum glaciation in Iberia, Italy, and the southern Dinarides (mainly Greece) lack precise chronology to pin it to the LGM, but for the Alps it is known that the maximum extent of glaciers occurred simultaneously with that of the northern hemisphere in the LGM (Reille and Andrieu, 1995). Nevertheless, in the northern Pyrenees, glaciers were less far extended during the LGM than during earlier cold spells in the Wuermian (García-Ruiz et al., 2003) and this seems to apply throughout Iberia (Reuther et
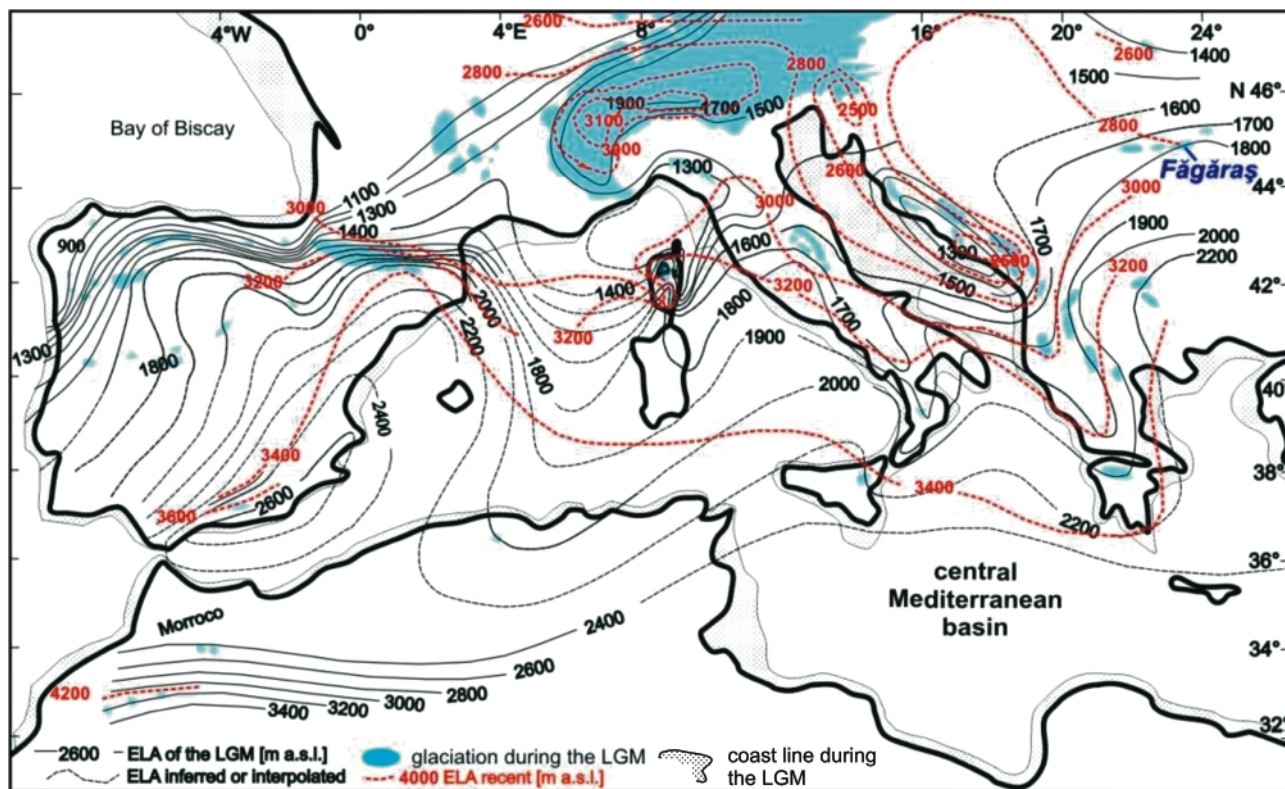

Figure 7: Mediterranean ELA of the LGM and the present (modified after Kuhlemann et al., 2008, recent ELA estimate largely after Messerli 1967).

al., 2007). In the western Southern Carpathians, the age of a stronger advance, early in the Wuermian or in the penultimate glaciation is yet unknown (Reuther et al., 2007; for Ukrainian Carpathians see also Rinterknecht et al., 2012). In northern Greece, maximum glacier extent in the Wuermian occurred during the LGM (Boenzi and Palmentola, 1997; Woodward et al., 2004). Older ELA maps for Greece and southern Italy show the maximum expansion in the Wuermian (Giraudi, 2004), not necessarily strictly within the LGM. A map (Fig. 7) comparing the modern ELA with that of the LGM highlights strong changes of regional gradients but only moderate changes of the pattern (modified from Kuhlemann et al., 2008).

6.1 Scenario for atmospheric flow during LGM and the late Wuermian

We assume considerable cyclonic activity in the western Mediterranean during the LGM, but not a dominant zonal track of storms across the basin. Today, fast-moving Atlantic disturbances rush eastward through the Mediterranean basin and southeastern Europe and cause moderate precipitation that increases with elevation. In the southern Balkan peninsula, LGM cyclone tracks may have followed modern tracks across and around southern Greece (Peloponnese) and across Montenegro, turning northward in the Vardar depression, triggered by the polar front (Fig. 8). Such cyclone tracks, however, are typical for the southern Balkan Peninsula in various modes of atmospheric circulation. In Romania, increased winter precipitation between 1960 and 1990 is correlated with eastern Atlantic blocking and enhanced Mediterranean cyclone activity (Tomozeiu et al., 2005). As a result, the Transylvanian basin is less sensitive to precipitation changes than the Dacian basin south of the Southern Carpathians (Tomozeiu et al., 2005).

With an LGM polar front on average located further south (COHMAP, 1988), southeast-directed passage of polar front cyclones from the eastern Atlantic ocean and their perturbations into the Mediterranean would cause outbreaks of polar air into the Gulf of Lions (Fig. 7, 8) more frequently than at present (Kageyama et al., 2006). Frequent distinctly meridional circulation during cold seasons with high synoptic activity and strong impact, as reflected by the LGM ELA pattern, may have alternated with zonal circulation and calm activity during warm seasons, which in the average of a LGM year may even have been the dominant mode, as inferred from the high-resolution climate model HadRM (Jost et al., 2005). Polar air masses invading the western Mediterranean basin typically pass through the funnel between the Alps and the Pyrenees (Rohling et al., 1998; Cacho et al., 2002). The Alps are forming the larger barrier, particularly when strongly glaciated in the LGM, and thus air masses breaking through the funnel diverged, preferentially turned left and frequently produced a cyclonal vortex in the rear of the Alps in the Gulf of Genoa. Cyclones born here then appear to have followed modern tracks to the southeast and east, affecting the study region, and unusual tracks along the Adriatic coast, directly moving towards the Alps.

Meridional atmospheric flow would be favoured by a low pressure gradient between the Azores high and the Iceland low pressure cells. The regional effect in western-central Europe is enhanced if interannual variation favours a negative mode in winter and a positive mode in summer (Cassou et al., 2004). At present, a blocking N-directed high-pressure ridge between the Azores and Iceland triggers a roughly S-directed geostrophic flow of polar air on its eastern flank into the western Mediterranean (inverted Ω-setting). Such regional setting was more common in the late Little Ice Age than in the
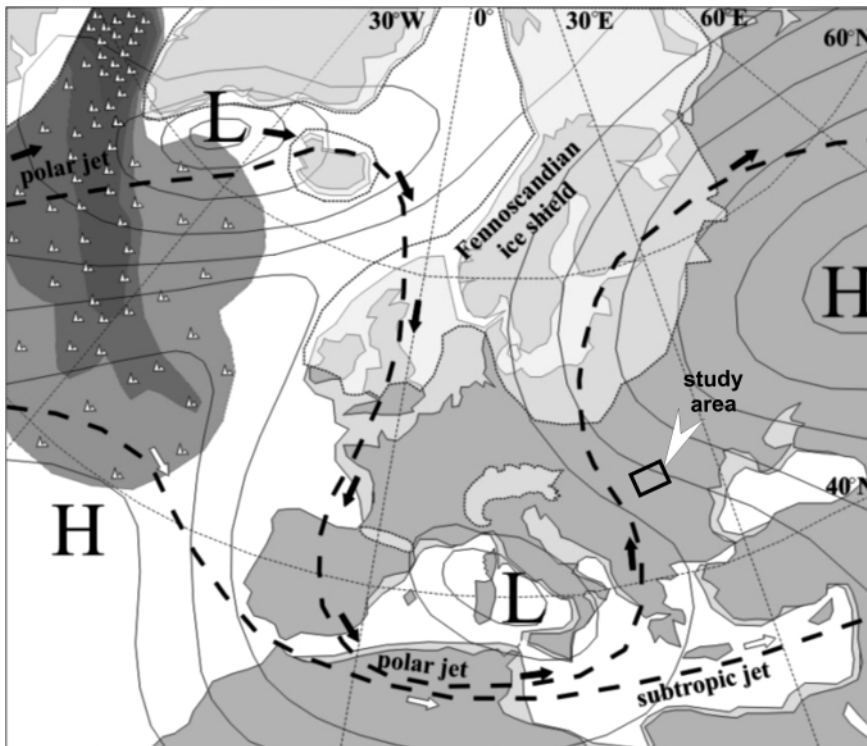

Figure 8: Sketch of the postulated typical winterly European atmospheric circulation in the LGM. Note that lines locating the subtropical and the polar jet stream shall reflect only a central line in a broad band of increased likelihood. The meandering jet streams of the Rossby waves are highly mobile. Flow of polar air in the higher atmosphere is indicated by black arrows whereas white arrows indicate the flow of subtropical air masses. White transparent flow lines indicate preferential cyclone tracks. Note that the study area (black rectangle next to white arrow) is situated close to a northeast-trending cyclone track which would trigger south to southwest winds prior to cyclone passage and cold westerly winds in its rear. The locations of high and low pressure cells as well as the isoline pattern are conceptual. Alternative proposals for better constrained cold spells of the Little Ice Age are discussed by Xoplaki et al. (2001). "H" means "High relative pressure", "L" means "Low pressure".

20th century (Jacobeit et al., 2001). As a result, polar air invading northwestern Africa likely caused dust storms and triggered cyclogenesis over the desert, as the polar jet came close to the subtropical jet stream. The subtropical jet stream probably triggered subtropic cyclones from the Atlantic to cross northernmost Africa like at present. As a consequence, desert air probably moved towards the NE, as indicated by the north-extending lobe of the ELA in southeastern Europe (Fig. 8). This is consistent with observations of enhanced wind-blown dust supply from the Sahara into the eastern Mediterranean during glacial times. Over relatively warm Mediterranean waters of the central and eastern basin, these NE-directed desert air masses would have mixed with the invading convective polar air masses and picked up additional moisture before moving northwards. During cold spells of the late glacial, this type of circulation apparently became less frequent, and in the early Holocene, the moisture transport pattern in southeastern Europe was already similar to the modern one.

7. Conclusions

Comparison of the recent and ancient snowline pattern during various cold spells, as preserved by terminal moraines deposited during glacier advances, yields information of preferential moisture transport. In a representative cross-section of the central South Carpathians, a disparity between slightly stronger southward glacier advance in the LGM and stronger northward advance in the Younger Dryas Stade and early Holocene suggests a disparity of moisture transport. In the LGM, moisture was preferentially advected from the southwest, whereas in the Younger Dryas Stade probably a quasi-modern almost symmetric precipitation pattern appeared. The west-east gradient found in the central South Carpathians indicates that in the western termination of the range this disparity is less strong, indicating that this region received more supply from the west. To explain preferential southwesterly moisture advection in the LGM, we have shown on the base of Mediterranean proxy-data that a meridional winterly LGM atmospheric circulation had stronger impact on the precipitation pattern than a zonal mode of circulation. However, the different atmospheric circulation in the LGM had less impact in the study region as compared to the western Mediterranean basin.

Acknowledgements

References

Balco, G., Stone, J., Lifton, N. and Dunai, T., 2008. A simple, internally consistent, and easily accessible means of calculating surface exposure ages and erosion rates from Be-10 and Al-26 measurements. Quaternary Geochronology 3, 174-195.

Bard, E., Rostek, F., Turon, J.-L. and Gendreau, S., 2000. Hydrological impact of Heinrich Events in the subtropical northeast Atlantic. Science 289, 1321-1324.

Bond, G., Showers, W., Cheseby, M, Lotti, R., Almasi, P., deMenocal, P., Priore, P., Cullen, H., Hajdas, I. and Bonani, G., 1997. A pervasive Millennial-scale cycle in North Atlantic Holocene and glacial climates. Science 278, 1257-1266.

Boenzi, F. and Palmentola, G., 1997. Glacial features and snow-line trends during the last glacial age in the Southern Apennines (Italy) and on Albanian and Greek mountains. Zeitschrift für Geomorphologie, N.F., Supplement-Band 41, 21-29.

Cacho, I., Grimalt, J.O., Canals, M., Sbaffi, L. Shackleton, N.J. Schönfeld, J. and Zahn, R., 2001. Variability of the western Mediterranean Sea surface temperature during the last 25,000 years and its connection with the Northern Hemisphere climatic changes. Paleoceanography 16, 40-52.

Cacho, I., Grimalt, J.O. and Canals, M., 2002. Response of the western Mediterranean Sea to rapid climatic variability during the last 50,000 years: a molecular biomarker approach. Journal of Marine Systems 33-34, 253-272.

Cassou, C., Terray, L., Hurrell, J.W. and Deser, C., 2004. North Atlantic winter climate regimes: spatial asymmetry, stationarity with time, and oceanic forcing. Journal of Climate 17, 1055-1068.

Chmeleff, J., von Blanckenburg, F., Kossert, K. and Jakob, D., 2010. Determination of the 10Be half-life by multicollector ICP-MS and liquid scintillation counting. Nuclear Instruments and Methods in Physics Research B263, 192-199.

COHMAP Members, 1988. Climate changes of the last 18'000 years: Observations and model simulations. Science 21, 1043-1052.

Constantin, S., Bojar A.V., Lauritzen, S.E. and Lundberg, J., 2006. Holocene Mediterranean continental environment: A speleothem record from Poleva Cave (Southern Carpathains, Romania). Paleogeography, Paleoclimatology, Paleoecology 243, 322-338.

Dunai, T.J., 2001. Influence of secular variation of the geomagnetic field on production rates of in situ produced cosmogenic nuclides. Earth and Planetary Science Letters 193, 197-212.

Florea, M., 1998. Munţii Făgăraşului. Studiu geomorphologic, Edit. Foton, Braşov, 114 pp.

Florineth, D. and Schlüchter, C., 1998. Reconstruction the Last Glacial Maximum (LGM) ice surface geometry and flowlines of the Central Swiss Alps. Eclogae Geologicae Helvetiae 9, 391-407.

Florineth, D. and Schlüchter, C., 2000. Alpine evidence for atmospheric circulation patterns in Europe during the Last Glacial Maximum. Quaternary Research 54, 295-308.

García-Ruiz, J.M., Valero-Garcés, B.L., Martí-Bono, C. and González-Sampériz, P., 2003. Asynchroneity of maximum glacier advances in the central Spanish Pyrenees. Journal of Quaternary Science 18, 61–72.

Giraudi, C., 2004. The Apennine glaciations in Italy. Quaternary Glaciations – Extent and chronology. In: Ehlers, J. and Gibbard, P.L. (Eds), Developments in Quaternary Sciences 2, 215-223.

Harrison, S., Yu, G. and Tarasov, P.E., 1996. Late Quaternary lake-level record from northern Eurasia. Quaternary Research 45, 138-159.

Hayes, A., Kucera, M., Kallel, N., Sbaffi, L. and Rohling, E.J., 2005. Glacial Mediterranean sea surface temperatures based on planktonic foraminiferal assemblages. Quaternary Science Reviews 24, 999-1016.

Horedt, H., 1988a. Rezente und eiszeitliche Schneegrenze in den Südkarpaten. Zeitschrift für Gletscherkunde 24/2, 177-192.

Horedt, H., 1988b. Asymmetrische Hangformen und Glatthangbildungen in den Südkarpaten. Zeitschrift für Geomorphologie N.F. 32/ 2, 231-238.

Hughes, P.D., 2010. Little Ice Age glaciers in Balkans: low altitude glaciation enabled by cooler temperatures and local topoclimatic controls. Earth Surface Processes and Landforms 35, 229-241.

Hughes, P.D. and Woodward, J.C., 2008. Timing of glaciation in the Mediterranean mountains during the last cold stage. Journal of Quaternary Science 23, 575-588.

Hughes, P.D., Gibbard, P.L. and Ehlers, J., 2013. Timing of glaciation during the last glacial cycle: evaluating the concept of a global 'Last Glacial Maximum' (LGM). Earth Science Reviews 125, 171-198.

Hughes, P.D., Woodward, J.C. and Gibbard, P.L., 2006. Glacial history of the Mediterranean mountains. Progress in Physical Geography 30, 334-364.

Ivy-Ochs, S., Kerschner, H. and Schlüchter, C., 2007. Cosmogenic nuclides and the dating of Lateglacial and Early Holocene glacier variations: The Alpine perspective. Quaternary International 164/165, 53-63.

Jacobeit, J., Jönsson, P., Bärring, L., Beck, C. and Ekström, M., 2001. Zonal Indices for Europe 1780–1995 and Running Correlations with Temperature. Climatic Change 48, 219-241.

Jost, A., Lunt, D., Kageyama, M., Abe-Ouchi, A., Peyron, O., Valdes, P.J. and Ramstein G., 2005. High-resolution simulations of the last glacial maximum climate over Europe: a solution to discrepancies with continental palaeoclimatic reconstructions? Climate Dynamics, DOI 10.1007/s00382-005-0009-4.

Kageyama, M., Lâıne, A., Abe-Ouchi, A., Braconnot, P., Cortijo, E., Crucifix, M., de Vernal, A., Guiot, J., Hewitt, C.D., Kitoh, A., Kucera, M., Marti, O., Ohgaito, R., Otto-Bliesner, B., Peltier, W.R., Rosell-Melé, A., Vettoretti, G., Weber, S.L., Yu, Y. and MARGO Project Members, 2006. Last Glacial Maximum temperatures over the North Atlantic, Europe and western Siberia: a comparison between PMIP models, MARGO sea-surface temperatures and pollen-based reconstructions. Quaternary Science Reviews 25, 2082–2102.

Kerschner, H. and Ivy-Ochs, S., 2007. Palaeoclimate from glaciers: Examples from the Eastern Alps during the Alpine Lateglacial and early Holocene. Global and Planetary Change 60, 58-71.

Kerschner, H. Kaser, G. and Sailer, R., 2000. Alpine Younger Dryas glaciers as palaeo-precipitation gauges. Annals of Glaciology 31, 80-84.

Kohl, C.P. and Nishiizumi, K., 1992. Chemical isolation of quartz for measurement of in-situ-produced cosmogenic nuclides. Geochimica and Cosmochimica Acta 56,3583-3587.

Korschinek, G., Bergmaier, A., Faestermann, T., Gerstmann, U. C., Knie, K., Rugel, G., Wallner, A., Dillmann, I., Dollinger, G., Lierse von Gestomski, C., Kossert, K., Maiti, M., Poutivtsev, M. and Remmert, A., 2009. A new value for the half-life of [10]Be by Heavy-Ion Elastic Recoil Detection and liquid scintillation counting. Nuclear Instruments and Methods in Physics Research B268, 187-191.

Kräutner, H.G., 1991. Pre-Alpine geological evolution of the East Carpathian metamorphics. Some common trends with the West Carpathians. Geologica Carpathica 42/4, 209-217.

Kräutner, H.G., 1997. Alpine and pre-Alpine terranes in the Romanian Carpathians and Apuseni Mts. Annales Géologiques des Pays Helléniques 37, 330–400.

Kubik., P.W. and Christl, M., 2010. [10]Be and [26]Al measurements at the Zurich 6 MV Tandem AMS facility. Nuclear Instruments and Methods in Physics Research B268, 880-883.

Kuhlemann, J., Van der Borg, K., Bons, P.D., Danišík, M. and Frisch, W., 2007. Erosion rates on subalpine paleosurfaces in the western Mediterranean by in-situ [10]Be concentrations in granites: implications for surface processes and long-term landscape evolution in Corsica (France). International Journal of Earth Sciences, doi: 10.1007/s00531-007-0169-z.

Kuhlemann, J., Krumrei, I., Rohling E., Kubik, P., Ivy-Ochs S. and Kucera, M., 2008. Regional synthesis of Mediterranean atmospheric circulation during the Last Glacial Maximum. Science 321, 1338-1340.

Kuhlemann, J., Milivojević, M., Krumrei, I. and Kubik, P., 2009b. Last glaciation of the Šara Range (Balkan peninsula): Increasing dryness from the LGM to the Holocene. Austrian Journal of Earth Sciences 102/1, 146-158.

Lehmann, P.W., 1881. Beobachtungen über Tektonik und Gletscherspuren im Fogaraschen Gebirge. Zeitschrift der Deutschen Geogischen Gesellschaft XXXIII, 109-117.

Lehmann, P.W., 1885. Die Südkarpaten zwischen Retjezat und Königstein. Zeitschrift der Gesellschaft für Erdkunde Berlin XX, 325-336.

Meland, M.Y., Jansen, E. and Elderfield, H., 2005. Constraints on SST estimates for the northern North Atlantic/ Nordic Seas during the LGM. Quaternary Science Reviews 24, 835–852.

Messerli, B., 1967. Die eiszeitliche und gegenwärtige Vergletscherung im Mittelmeergebiet, Geographica Helvetica 22, 105-228.

Mîndrescu, M., Evans, I.S. and Cox, N.J. 2010. Climatic implications of cirque distribution in the Romanian Carpathians: palaeowind directions during glacial periods. Journal of Quaternary Science. doi: 10.1002/jqs.1363.

Moser, F., Hann, H.P., Dunkl, I. and Frisch, W., 2005. Exhumation and relief history of the Southern Carpathians (Romania) as evaluated from apatite fission track chronology in crystalline basement and intramontane sedimentary rocks. International Journal of Earth Sciences 94, 218-230.

Nedelea, A., 2004. Valea Argeşului in sectorul montan – studiu geomorfologic. Thesis, 71 pp., Bucureşti.

Ohmura, A., Kasser, P. and Funk, M., 1992. Climate at the equilibrium line. Journal of Glaciology 38, 397-411.

Porter, S.C., 2001. Snow line depression in the tropics during the last glaciation. Quaternary Science Reviews 20/10, 1067-1091.

Posea, G., 1981. O singură glaciatiune in Carpati. Studii si Cercetari de Geol., Geofiz., Geogr., Geografie 18, 87-102.

Reille, M. and Andrieu, V., 1995. The late Pleistocene and Holocene in the Lourdes Basin, Western Pyrénées, France: new pollen analytical and chronological data. Vegetation History and Archeobotany 4, 1-21.

Reuther, A, Geiger, C., Urdea, P., Niller, H.-P. and Heine, K., 2004. Determing the glacial equilibrium line altitude (ELA) for the northern Retezat Mountains, Southern Carpathians and resulting paleoclimatic implications for the last glacial cycle. Ann. Univ. de Vest din Timişoara, Geografie, 14, 11-34.

Reuther, A, Urdea, P., Geiger, C., Ivy-Ochs, S., Niller, H.-P., Kubik, P. and Heine, K., 2007. Late Pleistocene glacial chronology of the Pietrele valley, Retezat Mountains, Southern Carpathians, constrained by 10Be exposure ages and pedological investigations. Quaternary International 164, 151-169.

Rinterknecht, V., Matoshko, A., Gorokhovich, Y., Fabel, D. and Xu, S., 2012. Expression of the Younger Dryas cold event in the Carpathian Mountains, Ukraine? Quaternary Science Reviews 39, 106-114.

Rohling, E.J., Hayes, A., Kroon, D., De Rijk, S. and Zachariasse, W.J., 1998. Abrupt cold spells in the NW Mediterranean. Paleoceanography 13, 316-322.

Sanders, C.A.E, Andriessen, P.A.M. and Cloetingh, S.A.P.L., 1999. Life cycle of the East Carpathian orogen; erosion history of a doubly vergent critical wedge assessed by fission track thermochronology. Journal of Geophysical Research, B, Solid Earth and Planets 104, 29095-29112.

Schildgen, T.F., Phillips, W.M. and Puves, R.S., 2005. Simulation of snow shielding corrections for cosmogenic nuclide surface exposure studies. Geomorphology 64, 67-85.

Severinghaus, J.P. and Brook, E.J., 1999. Abrupt Climate Change at the End of the Last Glacial Period Inferred from Trapped Air in Polar Ice. Science 286, 930-934.

Small, E.E., Anderson, R.S., Repka, J.L. and Finkel, R.,1997. Erosion rates of alpine bedrock summit surfaces deduced from in situ 10Be and 26Al. Earth and Planetary Science Letters 150, 413-425.

Stone, J., 2000. Air pressure and cosmogenic isotope production. Journal of Geophysical Research 105, 23753-23759.

Svendsen, J.I., and 29 coauthors, 2004. Late Quaternary ice sheet history of northern Eurasia. Quaternary Science Reviews 23, 1229–1271.

Tomozeiu, R., Stefan, S. and Busuioc, A., 2005. Winter precipitation variability and large-scale circulation patterns in Romania. Theoretical and Applied Climatology, doi 10.1007/s00704-004-0082-3.

Urdea, P., 1992. Rock glaciers and periglacial phenomena in the Southern Carpathians. Permafrost and Periglacial Processes 3, 267-273.

Urdea, P., 1997. Aspects concerning postglacial and present-day landforms evolution in Southern Carpathians. Acta Facultatis Rerum Naturalium Universitatis Comenianae Geographica 40, 107-117.

Urdea, P., 2000. Muntii Retezat. Studiu geomorphologie. Edit. Academiei, Bucureşti, 272 p. (in Romanian).

Urdea, P., 2004. The Pleistocene glaciation of the Romanian Carpathians. In: Ehlers, J. and Gibbard, P.L. (eds.), Quaternary Glaciations – Extent and chronology. Developments in Quaternary Sciences 2, 301-308.

Van Husen, D., 1997. Wuermian and late-glacial fluctuations in the Eastern Alps. In: Clapperton, C.M. (ed.), Fluctuations of local glaciers 30-8 ka BP. Quaternary International 38-39, 109-118.

Von Blanckenburg, F., Hewawasam T. and Kubik. P., 2004. Cosmogenic nuclide evidence for low weathering and denudation in the wet, tropical highlands of Sri Lanka. Journal of Geophysical Research 109, DOI: 10.1029/2003JF000049.

Woodward, J.C., Macklin, M.G. and Smith, G.R., 2004. Pleistocene glaciation in the mountains of Greece. In: Ehlers, J. and Gibbard, P.L. (Eds), Quaternary Glaciations – Extent and chronology. Developments in Quaternary Sciences 2, 155-173.

Xoplaki, E., Maheras, P. and Luterbacher, J., 2001. Variability of climate in meridional Balkans during the periods 1675-1715 and 1780-1830 and its impact on human life. Climate Change 48, 581-615.

Zemp, M., Hoelzle, M. and Haeberli, W., 2007. Distributed modelling of the regional equilibrium line altitude of glaciers in the European Alps. Global and Planetary Change 56, 83-100.

Zweigel, P., Ratschbacher, L. and Frisch, W., 1998. Kinematics of an arcuate fold–thrust belt: the southern Eastern Carpathians (Romania). Tectonophysics 297, 177–207.

Joachim KUHLEMANN[1)2)*)], Florentina DOBRE[2)], Petru URDEA[3)], Ingrid KRUMREI[2)], Emil GACHEV[4)], Peter KUBIK[5)] & Meinert RAHN[1)]

[1)] Swiss Nuclear Safety Inspectorate ENSI, Industriestrasse 19, 5200 Brugg, Switzerland;

[2)] Institute for Geosciences, University of Tübingen, Tübingen, Germany;

[3)] Department of Geography, West University of Timisoara, Romania;

[4)] Department of Geography, Ecology & Environment protection, SW University Blagoevgrad, Bulgaria;

[5)] Laboratory of Ion Beam Physics, ETH Zürich, Zürich, Switzerland;

[*)] Corresponding author, kuj@ensi.ch